

Structure and dynamical properties during solidification of liquid aluminum induced by cooling and compression

Min Wu(吴旻), Yong-Qi Yang(杨永琪), and Yao Wang(王垚)

Citation: Chin. Phys. B, 2024, 33 (**7**): 076301. DOI: 10.1088/1674-1056/ad39d0
Journal homepage: http://cpb.iphy.ac.cn; http://iopscience.iop.org/cpb

What follows is a list of articles you may be interested in

Ab initio nonadiabatic molecular dynamics study on spin—orbit coupling induced spin dynamics in ferromagnetic metals

Wansong Zhu(朱万松), Zhenfa Zheng(郑镇法), Qijing Zheng(郑奇靖), and Jin Zhao(赵瑾)
Chin. Phys. B, 2024, 33 (**1**): 016301. DOI: 10.1088/1674-1056/acf91d

Unveiling phonon frequency-dependent mechanism of heat transport across stacking fault in silicon carbide

Fu Wang(王甫), Yandong Sun(孙彦东), Yu Zou(邹宇), Ben Xu(徐贲), and Baoqin Fu(付宝勤)
Chin. Phys. B, 2023, 32 (**9**): 096301. DOI: 10.1088/1674-1056/acdfc0

Electronic structures and energy band properties of Be- and S-doped wurtzite ZnO

Zheng Shu-Wen (郑树文), Fan Guang-Han (范广涵), He Miao (何苗), Zhang Tao (张涛)
Chin. Phys. B, 2014, 23 (**6**): 066301. DOI: 10.1088/1674-1056/23/6/066301

Effect of Gd doping on the magnetism and work function of $Fe_{1-x}Gd_x$/Fe (001)

Tang Ke-Qin (汤可嵚), Zhong Ke-Hua (钟克华), Cheng Yan-Ming (程燕铭), Huang Zhi-Gao (黄志高)
Chin. Phys. B, 2014, 23 (**5**): 056301. DOI: 10.1088/1674-1056/23/5/056301

Investigations of high-pressure and high-temperature behaviors of the newly-discovered willemite-Ⅱ and post-phenacite silicon nitrides

Chen Dong (陈东)
Chin. Phys. B, 2013, 22 (**12**): 126301. DOI: 10.1088/1674-1056/22/12/126301

Structure and dynamical properties during solidification of liquid aluminum induced by cooling and compression

Min Wu(吴旻)[1,2], Yong-Qi Yang(杨永琪)[1], and Yao Wang(王垚)[1,†]

[1] *College of Materials Science and Engineering, Zhejiang University of Technology, Hangzhou* 310014, *China*
[2] *Shaoxing Research Institute, Zhejiang University of Technology, Shaoxing* 312000, *China*

(Received 1 February 2024; revised manuscript received 27 March 2024; accepted manuscript online 3 April 2024)

The structural transformation from a liquid into a crystalline solid is an important subject in condensed matter physics and materials science. In the present study, first-principles molecular dynamics calculations are performed to investigate the structure and properties of aluminum during the solidification which is induced by cooling and compression. In the cooling process and compression process, it is found that the icosahedral short-range order is initially enhanced and then begin to decay, the face-centered cubic short-range order eventually becomes dominant before it transforms into a crystalline solid.

Keywords: first-principles method, molecular dynamics, short-range order, liquid aluminum

PACS: 63.20.dk, 31.15.xv, 75.40.–s, 61.20.Ja **DOI:** 10.1088/1674-1056/ad39d0

1. Introduction

Understanding the structures and properties of disordered systems, such as metallic glasses and liquids, have been one of the most challenging topics in condensed matter physics.[1–5] In experiment, there is much less structural information of the disordered structure can be obtained by x-ray diffraction. However, first-principles molecular dynamics (FPMD) calculations can provide detailed microstructural information at an atomic level and have been proven to be able to explain the temperature- or pressure-dependent behaviors of disordered systems.[6,7] Due to the similarities in structures between liquids and metallic glasses, studying the structures and properties of liquids under pressure is an alternative approach to understanding the metallic glass counterparts. The experiment has confirmed that monatomic metallic glasses can be obtained from monatomic metallic liquids at ultra-high quench rates.[8]

Aluminum, as a widely used material in our daily life and industries, has been extensively studied both experimentally[9–11] and theoretically.[12–16] Boehler and Ross studied the melting curve of aluminum compressed to 80 GPa by using DAC.[9] Hänström and Lazor measured the melting curve of aluminum up to 50 GPa by using the same method.[10] It was shown that the melting temperature of aluminum increases linearly with pressure rising. A melting rate of 60 K/GPa was determined at ambient pressure, and at higher pressures, the melting rate decreased steadily to 50 K/GPa at 10 GPa. Jakse and Pasturel reported the temperature dependence of the self-diffusion coefficient and viscosity by *ab initio* molecular dynamics calculations of the structural and dynamical properties of liquid aluminum.[12] Sun *et al*. performed molecular dynamics simulations to study the effects of Mg and Sm dopants on the crystal nucleation in aluminum.[13] Kbirou *et al*. studied the effect of cooling rate on the evolution of atomic structure in aluminum monatomic metallic glass during the cooling process.[14]

However, the previous studies usually consider either temperature effect or pressure effect on the structure and properties of the molten Al. The similarity and correlation between the temperature and pressure effect have hardly been considered before. In the present study, the cooling and compression induced solidification of the molten aluminum are simulated by the first-principles molecular dynamics method. In cooling and compression induced solidification, it is found that the icosahedral short-range order (SRO) is initially enhanced. After the turning point, the icosahedral SRO starts to decay and the molten Al structure eventually transforms into a crystalline solid. The present results can be generalized in order to understand the effects of temperature and pressure on the structures and properties of other disordered systems.

2. Computational method

FPMD calculations and electronic structure calculations were performed by using the Vienna *Ab Initio* Simulation Package (VASP) based on the density functional theory.[17,18] The wave functions were represented by a plane-wave basis set with an energy cutoff of 400 eV. Effects of the core electrons were replaced by atomic projected augmented wave (PAW) potentials.[19] The Perdew–Burke–Ernzerhof (PBE) exchange–correlation functional was used.[20] Only Gamma point was used for the Brilllouin zone sampling. Valence electronic configurations of $3s^2 3p^1$ were used for the aluminum atomic potentials. In this work, the face-centered cubic unit cell of Al with spacegroup $Fm\bar{3}m$ which contains 4 atoms is

†Corresponding author. E-mail: wangyao@zjut.edu.cn

© 2024 Chinese Physical Society and IOP Publishing Ltd

used for the structural model construction. A $3 \times 3 \times 3$ supercell with 108 Al atoms is utilized as the a structural model for the subsequent molecular dynamics calculations. In the molecular dynamics calculations, the structure is heated up to 2000 K to generate the molten Al structure. After that, the supercell volume decreases step by step to generate the molten structures under different pressures. While in the cooling process, the temperature decreases from 2000 K to 600 K in several steps. For each step in both cooling calculation and compression calculation, the molecular (MD) runs with a canonical ensemble (NVT) (NVT represents constant particle number, constant volume, and constant temperature) for at least 60 ps.[21–23] The Nose–Hoover thermostat used to control the temperature.[22]

3. Results and discussion

3.1. Equation of state

The calculated equation of state for liquid aluminum during cooling at ambient pressure is shown in Fig. 1(a), with some cited experimental results for comparison. Apparently, our calculated results accord well with the experiments. For instance, Assael *et al*.'s experimental work reported that the density of the liquid aluminum at 0 GPa and 1000 K is about 2.36 g/cm^3,[24] which is very close to a value of 2.35 g/cm^3 in the present study. Sarou-Kanian *et al*. reported a value of $\sim$ 2.08 g/cm^3 for the liquid aluminum at 0 GPa and 2000 K,[25] which is comparable to a value of 2.09 g/cm^3 in the present study under the same P, T conditions. Malyshev *et al*. suggested a cluster-associate model of the temperature dependence of the aluminum density, $\rho = 2368(933/T)^{0.109575(1073/T)^{-0.991033}}$ kg/m^3.[26] At several selected temperatures, the densities calculated from this model are very consistent with our results.

The pressure-dependent equations of state of liquid aluminum at temperatures of 1000 K and 2000 K are shown in Figs. 1(b) and 1(c), respectively. At 1000 K, the density of the liquid Al increases almost linearly with pressure rising, while the bulk modulus increases from 37.50 GPa to 60.99 GPa. When the pressure increases up to 5.49 GPa, the liquid structure solidifies and becomes a crystal. In the recent experiments by Hänström and Lazor, it was found that the melting point of aluminum at 5.49 GPa is about 1008.76 K, which is consistent with our calculation result.[10] At 2000 K, the Al liquid state is still kept in a much larger pressure range than 1000 K. The liquid structure shows a larger compressibility at low pressure. When the pressure increases up to 29.90 GPa, it transforms into a crystalline solid.

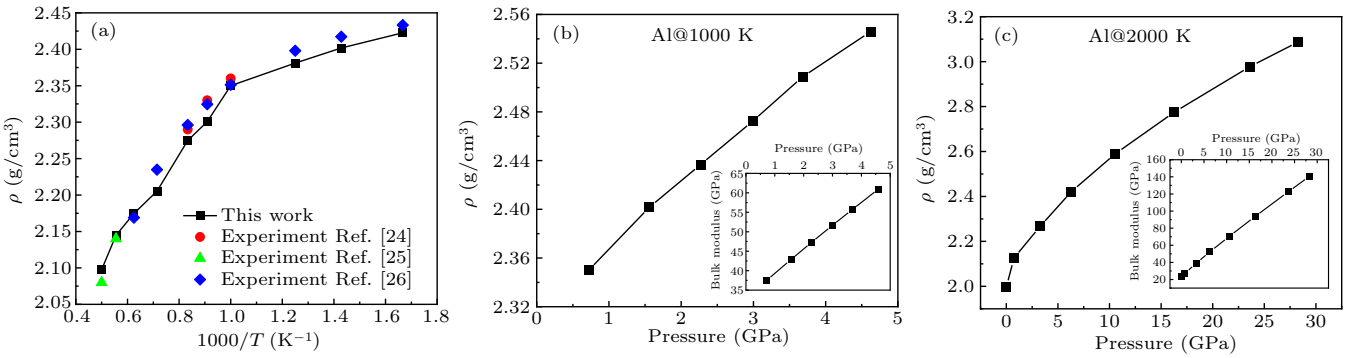


Fig. 1. (a) Equation of state of liquid aluminum during cooling from 2000 K to 600 K. (b) Equation of state of liquid aluminum during compression at 1000 K. (c) Equation of state of liquid aluminum during compression at 2000 K. Insets show pressure-dependent bulk modulus.

3.2. Atomic cluster alignment analysis

The atomic cluster alignment (ACA) method is employed to study the microstructural evolution from a liquid to a crystalline solid in the cooling process and the compression process. The atomic clusters extracted from the MD trajectories contains the nearest neighbor atoms, so the aligned clusters can intuitively present the SRO of the liquid structures.[27,28] Figure 2(a) shows the ACA results of the liquid aluminum in the cooling process. At 1400 K, the structure is highly disordered and the aligned cluster shows no SRO. At 1200 K–1000 K, the SRO starts to appear and is similar to the icosahedral pattern. This is consistent with the Frank's hypothesis[29] that icosahedron may be the dominant arrangement in monatomic liquids. Moreover, such icosahedral SROs are also commonly found in metallic glasses which are usually formed by fast cooling process.[30] When the temperature decreases to 600 K, a clear crystalline pattern is achieved, indicating that the structure is solidified. These structural evolutions can also be found in the relative energy values of those 4 templates. The "relative energy" represents the degree of similarity between the atomic clusters and the templates. The lower value of the "relative energy" represents the higher similarity of the atomic clusters to the template clusters.[28] At 1400 K, the relative energy values of 4 templates are close to each other. It means no SRO is dominant in such disordered liquid structures. At 1200 K, the "relative energy" of the icosahedral template is clearly lower than those of the other three templates, indicating that the icosahedral SRO starts to be-

come the major feature of the whole structure. At 1000 K, the icosahedral SRO increases further. However, when the temperature decreases further to 800 K, the icosahedral SRO starts to decay. At 600 K, the FCC SRO becomes dominant which is consistent with the patterned atomic configuration. As a reference, Fang *et al*. showed that the liquid aluminum is solidified at 800 K in the cooling process.[27] The difference in solidification temperature may be affected by the initial temperature of liquid aluminum or the cooling rate. Li *et al*. suggested that as the initial temperature of a metallic liquid decreases, its freezing pointlowers accordingly.[31]

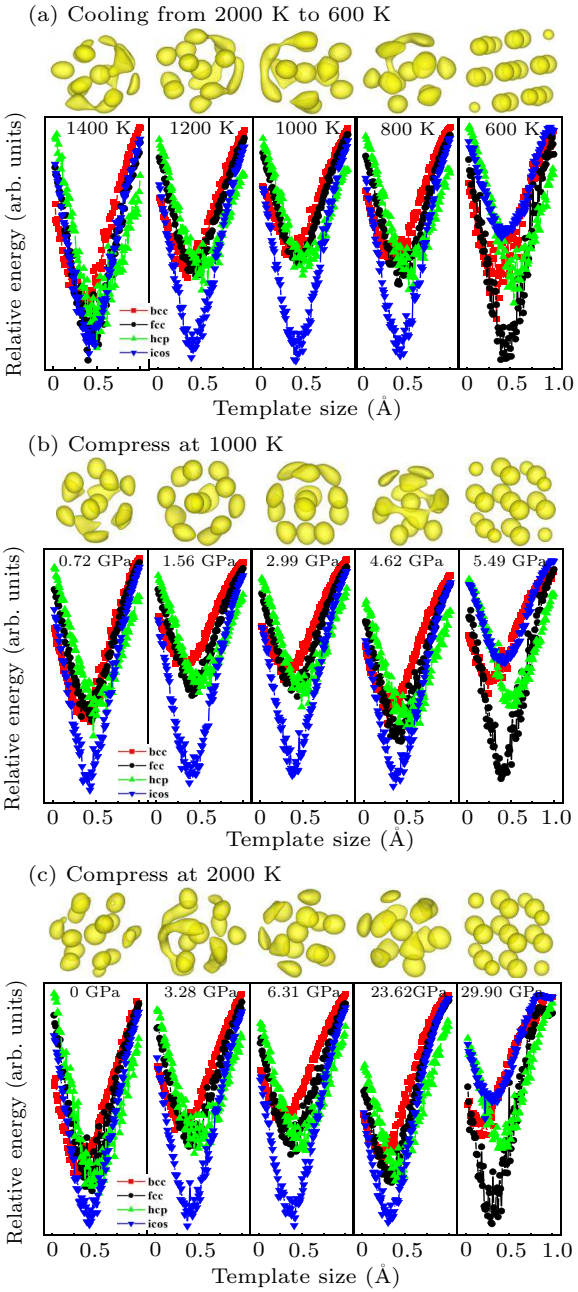


Fig. 2. Atomic cluster alignment analysis of liquid aluminum during cooling and compression, respectively, showing (a) cooling at ∼ 0 GPa. (b) compression at 1000 K, and (c) compression at 2000 K.

As is well known, with temperature lowering in the cooling process, the kinetic energy values of the atoms in the liquid structure decrease. On the other hand, compression can also be considered as an alternative tool to restrict atomic motion in liquid structure. It is interesting to compare the temperature effect with pressure effect on the structural evolution during the solidification. The ACA results of the liquid aluminum under compression at 1000 K and 2000 K are shown in Figs. 2(b) and 2(c), respectively. Interestingly but not surprisingly, the compression effect on the SRO seems to be similar to the cooling effect. At 0 GPa and 2000 K, the Al liquid structure is highly disordered and no clear SRO can be found. There is no dominant pattern that can be seen in the "relative energy" plot. When the compression starts, the icosahedral SRO starts to become dominant at least in the pressure ranging from 3.28 GPa to 6.31 GPa. With further compression, the icosahedral SRO starts to decay and its "relative energy" becomes closer to the counterparts of other templates. When the pressure increases to 29.9 GPa, the Al liquid structure solidifies and becomes a crystal. It should be noticed that the packing efficiency of the icosahedron is about 0.84,[32] which is higher than a value of 0.74 for the FCC structure. This can be the reason for the icosahedral SRO increasing initially by compression which tends to form a denserpacked structure. With further compression, when there are no more icosahedrons to form, the existing icosahedrons will deform in order to be packed more densely with further compressing. As a result, the icosahedral SRO starts to decay and becomes less dominant with further compression. Eventually, the pressure effect turns the Al liquid structure into a most densely packed crystalline solid.

It should be also noticed that the cooling process and compression process show similar effects on the structural evolution during the solidification, but it is not always the case. For instance, it has been reported that the liquid monoatomic metal can be quenched into metallic glass with ultrafast cooling rate.[8] It can be expected that the liquid structure will be solidified into a glass state by ultrafast cooling, but unlikely by compression. With ultrafast cooling, the quenched atoms have no kinetic energy enough to overcome the energy barrier to become a crystal, so they remain in a glass state. However, the compressed atoms usually have enough time for optimization, and most likely the monoatomic metal structure will densely packed and becomes a crystal.

3.3. Radial distribution functions

Figure 3(a) shows the radial distribution function (RDF) of the aluminum structure in the cooling process. The first peak gradually sharpens as the temperature decreases, demonstrating the presence and enhancement of SRO during solidification. The distinct second peak appears at 600 K, indicating that the system has crystallized. Atomic coordination number (CN) can be used to analyze the local structural characteristics

of liquid aluminum in the cooling process and compression process. The cutoff radius is chosen to be corresponding to the first peak position of the RDF. It should be noted that in order to better describe the structural evolution, the CN analysis in these structures at different temperatures or pressures should be combined with other structural analysis such as RDF and ACA (atomic cluster alignment) methods as performed in the present work. As shown in Fig. 3(b), the CN of liquid aluminum continues to increase with temperature decreasing, for the contraction of the volume leads to a denser structure and smaller spacing of the Al atoms.

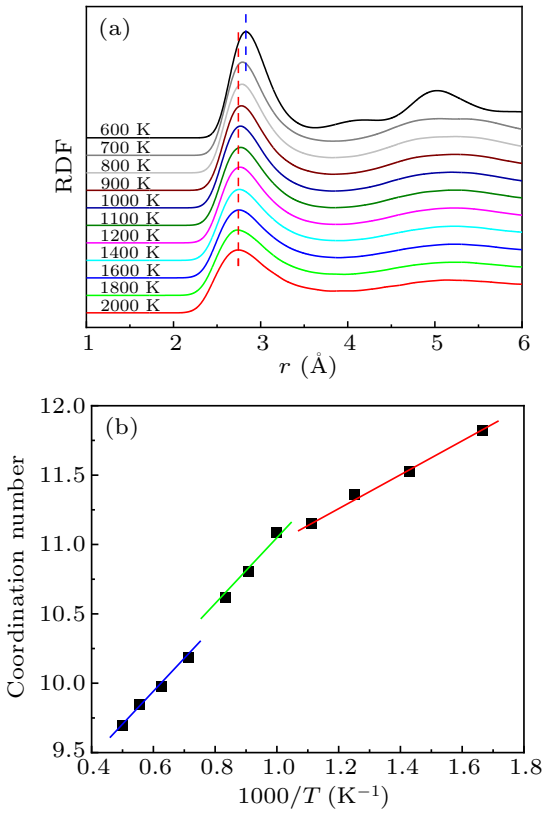


Fig. 3. (a) Radial distribution function for liquid aluminum at various cooling temperatures, showing that cutoff radii appearing at the first peak position of the RDF at 2000 K. (b) The temperature-dependent coordination number of liquid aluminum.

The pressure-dependent radial distribution functions (RDFs) of liquid aluminum at 1000 K and 2000 K are shown in Figs. 4(a) and 4(b), respectively. At 1000 K, the first peak of the RDF is very sharp and located at $\sim$ 2.77 Å under 0.72 GPa, while the second peak is very weak, which indicates that the liquid structure is highly disordered. The system becomes denser and denser under compression, the positions of the first peak shifts toward smaller value in the compression process, and the second peak becomes more and more prominent as shown in Fig. 4(a). The same trend is observed for the RDF at 2000 K as can be seen in Fig. 4(b). The first peak is located at $\sim$ 2.75 Å under 0 GPa. The liquid aluminum has the same change tendency at 1000 K and 2000 K. Also the second peak becomes sharp and the first peak shifts toward smaller value when liquid aluminum is crystallized. The CN of liquid aluminum atoms in the compression process at 1000 K and 2000 K are shown in Fig. 4(c). In the initial stage of compression, the aluminum atoms are squeezed to form an icosahedral SRO, which has a maximum local packing efficiency and leads the CN to increase significantly. With further compression, the icosahedral SRO starts to decay, and the CN increases slower with the pressure rising. The CN increases abruptly when the liquid aluminum is crystallized.

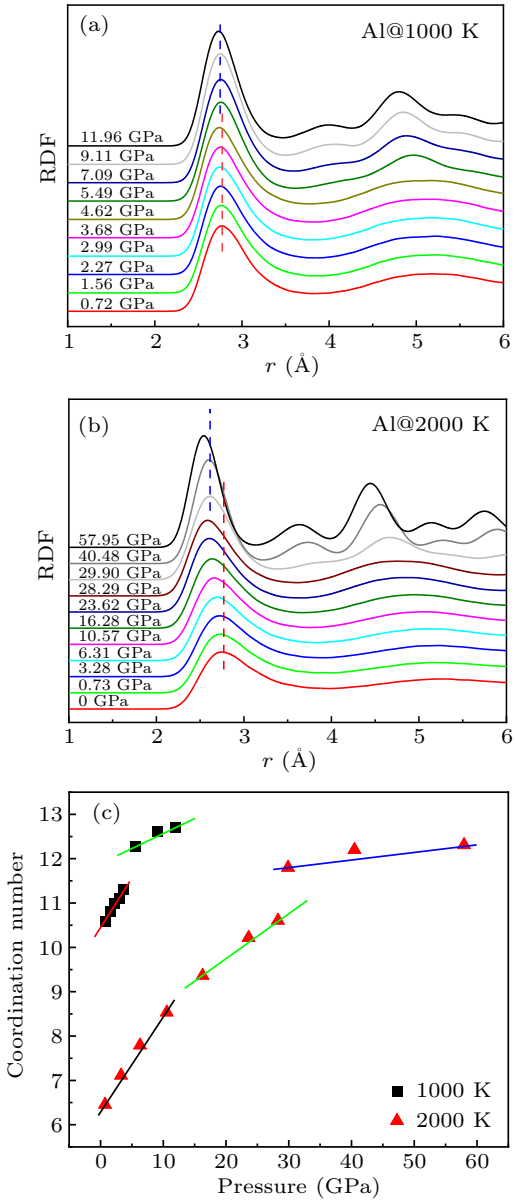


Fig. 4. Pressure-dependent radial distribution function for liquid aluminum at (a) 1000 K and (b) 2000 K, with cutoff radii being at the first peak position of RDF at 0.72 GPa for 1000 K and 0 GPa for 2000 K, respectively. (c) Curve of pressure-dependent coordination number of liquid aluminum at 1000 K and 2000 K.

3.4. Diffusivities and viscosities

Self-diffusion coefficient and viscosity are the main parameters describing the kinetic properties of liquid structures. The self-diffusion coefficient D of aluminum atoms in the liquid structure is calculated according to the Einstein's mean

square displacement equation

$$D = \frac{1}{N}\sum_{i=1}^{N}\frac{\langle r_i(t) - r_i(0)\rangle^2}{6t},$$

where r_i is the position of atom i and $\langle\ \rangle$ denotes the average value of the coefficients at many time origins. The calculation of the self-diffusion coefficient D in the cooling process is shown in Fig. 5(a). During the initial stage of the cooling process, the self-diffusion coefficient of liquid aluminum rapidly decreases from 2.12×10^{-8} m^2·s^{-1} at 2000 K to 0.55×10^{-8} m^2·s^{-1} at 1000 K, which are in agreement with the calculations of Jakse and Pasturel,[12] and Nenuwe and Osafile.[33] The calculated results are slightly lower than the experimental values measured by Demmel *et al.*[34] With further cooling, the self-diffusion coefficient of liquid aluminum decreases to 0.24×10^{-8} m^2·s^{-1} at 700 K. The liquid aluminum is crystallized at 600 K and the aluminum atoms almost cease to diffuse.

The results of the self-diffusion coefficient D at 1000 K and 2000 K are shown in Figs. 5(c) and 5(e), respectively. At 1000 K, during the initial compression stage, the calculated self-diffusion coefficient decreases rapidly from 0.54×10^{-8} m^2·s^{-1} at 0.72 GPa to 0.46×10^{-8} m^2·s^{-1} at 2.27 GPa, very close to 0.68×10^{-8} m^2·s^{-1} calculated by Alemany *et al.* at ambient pressure and 1000 K.[35] With further compression, the self-diffusion coefficient decreases from 0.39×10^{-8} m^2·s^{-1} at 2.99 GPa to 0.34×10^{-8} m^2·s^{-1} at 4.62 GPa. Until the liquid aluminum is crystallized, the aluminum atoms no longer diffuse. At 2000 K, the self-diffusion coefficient decreases from 2.44×10^{-8} m^2·s^{-1} at 0 GPa to 1.67×10^{-8} m^2·s^{-1} at 3.28 GPa during the initial compression stage. Then, the self-diffusion coefficient only decreases from 1.32×10^{-8} m^2·s^{-1} at 6.31 GPa to 0.39×10^{-8} m^2·s^{-1} at 28.29 GPa. This may be influenced by the distance between the Al atoms. These are consistent with the results of the P–ρ equation of state mentioned above. At 29.9 GPa, the aluminum atoms in the system almost no longer diffuse, indicating that the liquid aluminum is crystallized. Compared with the results of the self-diffusion coefficient at 1000 K, the self-diffusion coefficient of aluminum at the initial stage of compression at 2000 K is higher, about five times higher than that at 1000 K.

The viscosity of the liquid aluminum is calculated from the Stokes–Einstein equation[36] and the Green–Kubo relationship,[37] in which the Stokes–Einstein equation uses the self-diffusion coefficient in the form of $\eta_{SE} = (k_B T)/(2\pi D d)$, with η_{SE} being the viscosity, d the effective atomic diameter, T the temperature, and k_B the Boltzmann constant. The Green–Kubo relationship uses a time-dependent function of the temporal stress tensor from MD calculations, calculated from the following equations:

$$\eta_{GK} = \frac{V}{k_B T}\int_0^\infty \langle P_{xy}(t)P_{xy}(0)\rangle\,\mathrm{d}t,$$

where η_{GK} is the viscosity, V the volume of the system, $\langle\ \rangle$ the system averaging, and P_{xy} the non-diagonal component of the instantaneous stress tensor. The results, calculated from the Stokes–Einstein equation and the Green–Kubo relation, are shown in Fig. 5(b). The viscosities, calculated by using both methods, increase almost linearly with temperature and remain below 2.50 mPa·s until crystallization. And the calculated results are in good agreement with those of both Jakse and Pasturel[12] and Nenuwe and Osafile.[33]

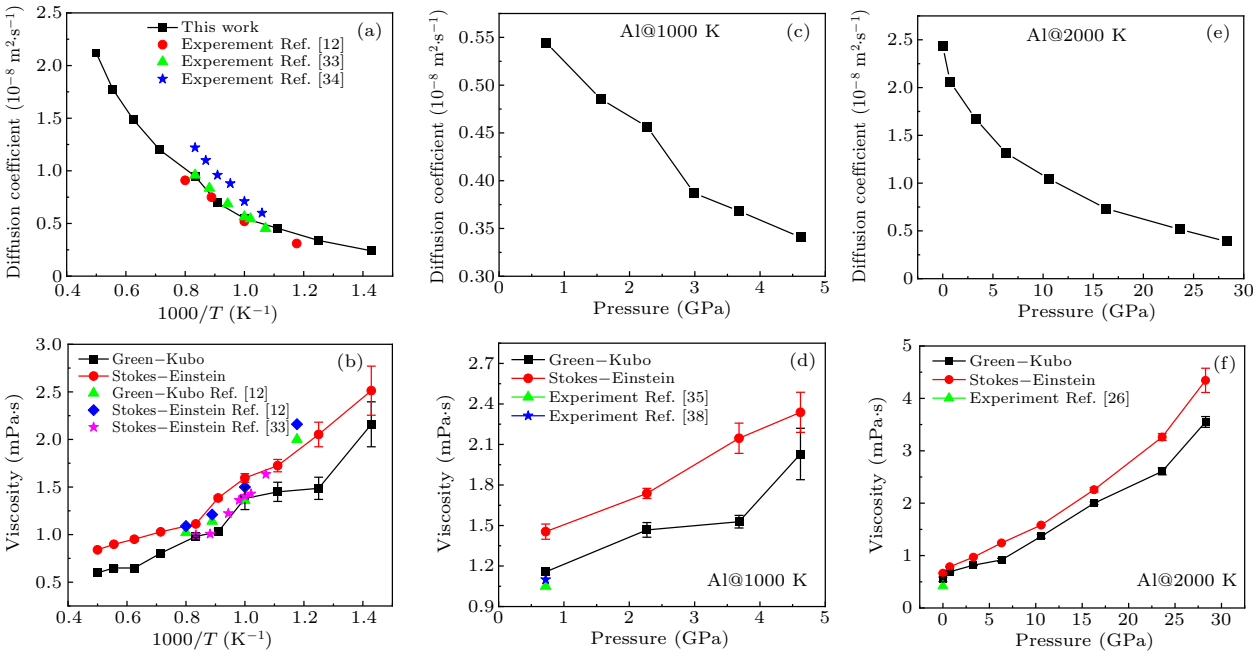


Fig. 5. Self-diffusion coefficients of liquid aluminum varying with (a) cooling temperature, pressure at (c) 1000 K and (e) 2000 K. Viscosities of liquid aluminum, calculated by using the Stokes–Einstein equation and the Green–Kubo relation, varying with (b) cooling temperature, pressure at (d) 1000 K and (f) 2000 K.

The viscosities of liquid aluminum at 0.72 GPa and 1000 K, calculated from the Stokes–Einstein equation and the Green–Kubo relation, are 1.61 mPa·s and 1.16 mPa·s, respectively, as shown in Fig. 5(d). This result is slightly higher than 1.05 mPa·s calculated by Alemany *et al*. by using the Stokes–Einstein equation at ambient pressure and 1000 K[35] and close to an experimental value of 1.10 mPa·s measured by Shimoji and Itami at ambient pressure and 990 K.[38] The viscosities of liquid aluminum at 0 GPa and 2000 K, calculated from the Stokes–Einstein equation and the Green–Kubo relation, are 0.73 mPa·s and 0.55 mPa·s, respectively, which are close to the value of 0.42 mPa·s calculated by Malyshev *et al*. at ambient pressure and 2000 K, as shown in Fig. 5(f).[26] The viscosities calculated by using both methods at a temperature of 1000 K increase linearly with pressure rising, and the viscosity value before curing of liquid Al is less than 2.20 mPa·s. The viscosities calculated by both methods at temperature 2000 K increase linearly with pressure, and none of the viscosity values before curing exceeds 3.60 mPa·s.

4. Conclusions

In this work, FPMD calculations are performed to study the structure of liquid aluminum in the cooling process and compression process. The results show that liquid aluminum undergoes a continuous liquid structural change during both cooling and compression, respectively. In the cooling process, liquid aluminum is crystallized at 600 K in the present study. An initial enhancement of the icosahedral SRO is found in the cooling process and the compression process at 1000 K and 2000 K. The increase in icosahedral SRO of liquid aluminum leads CN to increase rapidly and diffusion rate to decrease. With further cooling and compression, the icosahedral SRO starts to decay and becomes less dominant. Eventually, the liquid aluminum structure under cooling and compression is solidified and becomes a crystal. The viscosities obtained by using the Green–Kubo relationship and the Stokes–Einstein equation in the cooling process are in good agreement with the experimental results. The viscosities at 1000 K and 2000 K increase linearly with pressure. The present results not only reveal the structural and kinetic properties of liquid structure under pressure, but also can be extended to study the effects of temperature and pressure on the behaviors of other disordered systems.

Acknowledgements

Project supported by the National Natural Science Foundation of China (Grant No. 51701180) and the Foundation of the State Key Laboratory of Coal Conversion, China (Grant No. J22-23-103).

References

[1] Poole P H, Grande T, Angell C A and McMillan P F 1997 *Science* **275** 5298
[2] Mishima O and Stanley H E 1998 *Nature* **396** 6709
[3] Wilding M C, Wilson M and McMillan P F 2006 *Chem. Soc. Rev.* **35** 964
[4] Cheng Y Q and Ma E 2011 *Prog. Mater. Sci.* **56** 379
[5] Pan S P, Feng S D, Wang L M, Qiao J W, Niu X F, Dong B S, Wang W M and Qin J Y 2016 *Sci. Rep.* **6** 27708
[6] Wu M, Lou H. B, Tse J S, Liu H Y, Pan Y M, Takahama K, Matsuoka T, Shimizu K and Jiang J Z 2016 *Phys. Rev. B* **94** 054201
[7] Wu M, Liang Y F, Jiang J Z and Tse J S 2012 *Sci. Rep.* **2** 398
[8] Zhong L, Wang J W, Sheng H W, Zhang Z and Mao S X 2014 *Nature* **512** 7513
[9] Boehler R and Ross M 1997 *Earth Planet. Sc. Lett.* **153** 223
[10] Hänström A and Lazor P 2000 *J. Alloys Compd.* **305** 209
[11] Iqbal N, Dijk N H V, Verhoeven V W J, Montfrooij W, Hansen T, Katgerman L and Kearley G J 2003 *Acta Mater.* **51** 15
[12] Jakse N and Pasturel A 2013 *Sci. Rep.* **3** 3135
[13] Sun Y, Zhang F, Yang L, Song H J, Mendelev M I, Wang C Z and Ho K M 2019 *Phys. Rev. Mater.* **3** 023404
[14] Kbirou M, Trady S, Hasnaoui A and Mazroui M 2017 *Philos. Mag.* **97** 30
[15] Jakse N and Pasturel A 2013 *J. Phys.: Condens. Matter* **25** 285103
[16] Rueter H R and Redmer R 2014 *Phys. Rev. Lett.* **112** 145007
[17] Kresse G and Hafner J 1994 *J. Phys.: Condens. Matter* **6** 8245
[18] Kresse G and Joubert D 1999 *Phys. Rev. B* **59** 1758
[19] Blochl P E 1994 *Phys. Rev. B* **50** 17953
[20] Perdew J P, Burke K and Ernzerhof M 1996 *Phys. Rev. Lett.* **77** 3865
[21] Frenkel D, Smit B and Ratner M A 1997 *Phys. Today* **50** 66
[22] Car R and Parrinello M 1985 *Phys. Rev. Lett.* **55** 2471
[23] Truhlar D G 2010 *Phys. Today* **63** 54
[24] Assael M J, Kakosimos K, Banish R M, Brillo J, Egry I, Brooks R, Quested P N, Mills K C, Nagashima A, Sato Y and Wakeham W A 2006 *J. Phys. Chem. Ref. Data* **35** 285
[25] Sarou-Kanian V, Millot F and Rifflet J C 2003 *Int. J. Thermophys.* **24** 277
[26] Malyshev V P, Makasheva A M and Suleimenov T 2015 *Russian Metallurgy (Metally)* **2015** 443
[27] Fang X W, Wang C Z, Yao Y X, Ding Z J and Ho K M 2010 *Phys. Rev. B* **82** 184204
[28] Sun Y, Zhang F, Ye Z, Zhang Y, Fang X W, Ding Z J, Wang C Z, Mendelev M I, Ott R T, Kramer M J and Ho K M 2016 *Sci. Rep.* **6** 23734
[29] Frank F C 1952 *Proc. R. Soc. Lond. A* **215**
[30] Hirata A, Kang L J, Fujita T, Klumov B, Matsue K, Kotani M, Yavari A R and Chen M W 2013 *Science* **341** 6144
[31] Li G J, Wang Q, Cao Y Z, Lv X, Li D G and He Y C 2011 *Acta Phys. Sin.* **60** 093601 (in Chinese)
[32] Torquato S and Jiao Y 2009 *Phys. Rev. E* **80** 041104
[33] Nenuwe O N and Osafile O E 2018 *J. Appl. Sci. Environ. Manage.* **22** 519
[34] Demmel F, Szubrin D, Pilgrim W C and Morkel C 2011 *Phys. Rev. B* **84** 014307
[35] Alemany M M G, Gallego L J and González D J 2004 *Phys. Rev. B* **70** 134206
[36] Mason T G 2000 *Rheo. Acta* **39** 371
[37] Alfè D and Gillan M J 1998 *Phys. Rev. Lett.* **81** 5161
[38] Shimoji M and Itami T 1986 *Atomic Transport in Liquid Metals* (Trans. Tech. Publications Inc.) p. 122